Numerical Investigation for Combustion Characteristics of Vacuum Residue in a Test Furnace

S. Sreedhara*, Kang Y. Huh*† and Hoyoung Park**

ABSTRACT

It has become inevitable to search for alternative fuels due to severe energy crisis these days. Use of alternative fuels, which are typically of lower quality, tends to increase environmental pollution, including formation of nitrogen oxides (NOx). In this paper performance of vacuum residue has been investigated experimentally as well as numerically in typical operating conditions of a furnace. Heat release reaction is modeled as sequential steps of devolatilization, simplified gas phase reaction and char oxidation as that for pulverized coal. Thermal and fuel NOx are predicted by conditional estimation of elementary reaction rates and are compared against measured experimental data. On the overall reasonable agreement is achieved for spatial distributions of major species, temperature and NOx for all test cases.

Key words : Vacuum residue, Turbulent combustion, Conditional Moment Closure, NOx

1. Introduction

Urgent fuel crisis has forced us to look for alternative fuels not to compromise our current life standards. One of major research targets is utilization of different, cheaper fuels of lower quality. Special designs of furnaces or gasifiers are usually required to burn these unconventional fuels. Stringent restriction on pollutant formation made it mandatory to study the parameters affecting pollutant emission in detail. Among those pollutants nitrogen oxides have been considered as a severe threat to atmospheric environment.

Vacuum residue is a semi-liquid fraction of hydrocarbon which boils above 800 K. It has been mainly used to manufacture asphalt for road pavement [8]. It has also been used as a fuel for Integrated Gasification Combined Cycle (IGCC) world wide while the market potential for residue-based IGCC is anticipated to go up to 120 GW by the year 2010 [18]. In Japan 475 ton/hr-Vacuum Residue fired boiler began commercial operation in 1998 [7,14]. Vacuum residue is cheaper than heavy oil and has a typical composition of C:88.65 %, H:10.745 %, O:0.136 % and N: 0.469 % by mass. However, its application as fuel is still questionable because of the higher contents of nitrogen and sulphur, which contribute to higher levels of NOx and SOx emission.

Much work has been done on coal combustion by Smoot and co workers [5, 9, 15]. Combustion of extra heavy oil was recently investigated by Watanabe et.al [16].

* 포항공과대학교 기계공학과
† 연락저자, huh@postech.ac.kr
** 한국전력 전력연구원

They described the combustion process of heavy oil in the same way as that of coal [16]. First, the fuel goes through pyrolysis and devolatilization to produce fuel vapor. These vapors involve gas phase reaction while finally left solid carbon oxidizes to CO and CO_2. In this paper a similar approach is adopted for combustion of vacuum residue, while more sophisticated NO models based on the conditional moment closure (CMC) concept are incorporated.

2. Homogeneous NOx reactions

2.1 Thermal NO

Thermal NO is formed due to oxidation of atmospheric nitrogen at a relatively high temperature. It is formed in fuel lean environment with its mechanism described by the well-known Zeldovich steps [13] as follows.

$$N_2+O = NO+N \quad (1)$$
$$N+O_2 = NO+O \quad (2)$$
$$N+OH = NO+H \quad (3)$$

The overall reaction rate may be written as [4],

$$\frac{d[NO]}{dt} = 2[O]\left\{\frac{k_1[N_2]-k_{-1}k_{-2}[NO]^2}{1+\frac{k_{-1}[NO]}{k_2[O_2]+k_3[OH]}}\right\} \quad (4)$$

If initial concentrations of NO and OH are low, then the rate equation simplifies to

$$\frac{d[NO]}{dt} = 2k_1[O][N_2] \quad (5)$$

Concentration of the oxygen atom may be obtained from concentrations of the other major species by assuming 'partial equilibrium'.

$$[O] = K_{eq}\frac{[O_2][CO]}{[CO_2]} \quad (6)$$

Formation of thermal NO is very low at mean temperatures below 1600-1800 K [13]. It is also negligible at fuel-rich mixture because of absence of oxygen atoms.

2.2 Fuel NO

Presence of nitrogen in the fuel contributes significantly to total NO formation. It is referred to as fuel NO, which may sometimes be of the order of 75 - 95% [5, 9] out of total NO emission. The fuel nitrogen primarily evolves as HCN and also as NH3, to a lesser extent.

3. Experimental setup

Experimental work was carried out at Korea Electric Power Research Institute (KEPRI). The experimental furnace has the bore equal to 200 mm and the height equal to 3200 mm.

Table 1. Feed rates of fuel, air and steam for the test cases. Composition of Vacuum residue under present investigation is C: 85.30 %, H: 10.34 %, O: 0.13 %, N: 0.45 % and S: 3.78 %.

Test No.	Fuel feed rate in kg/hr	Air feed rate in m^3/hr	Steam feed rate in kg/hr
1	10.90	97.50	4.658
2	12.01	97.50	4.658
3	14.21	97.50	4.658

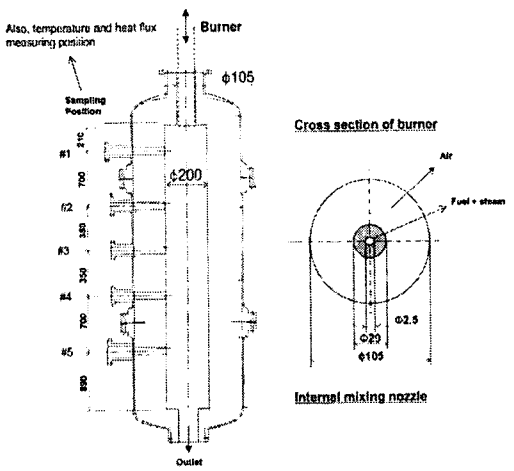

Fig 1. Details of furnace and burner in experiment.

Geometrical shapes of the furnace and the burner with a single nozzle are shown in Fig. 1. Nozzles of both internal and external mixing types are employed in the experiment. Three test cases are carried out by varying the fuel rate with an internal mixing type of nozzle. Details on the test cases are listed in Table 1. Gas samples are extracted at different axial and radial locations to obtain data for temperature and species mole fractions. Numerical simulations are performed for the same test cases in Table 1 as well.

4. Numerical simulation

A sixty degree (60) 3D sector mesh was used for numerical simulations with a periodic boundary conditions applied in the theta direction. Flow field is calculated by KIVA, an advantage of which is an open source code. The devolatilization process of fuel is modeled as

$$\frac{dV}{dt} = Aexp(-E/RT)(V_\infty - V) \quad (7)$$

where V_∞ is the total mass of volatiles at the beginning and V is the current mass of evaporated volatiles. Solid coke remains after evaporation of all volatiles. This solid coke oxidizes further to CO and CO_2 as follows [16]

$$C+(1-n/2)O_2 \rightarrow nCO+(1-n)CO_2 \quad (8)$$

where the value of 'n' is obtained from the following relationship [1].

$$\frac{n}{n-1} = 2500.exp\left(-\frac{6240}{T}\right) \quad (9)$$

The reaction model for coke gasification is given as [5]

$$\frac{dx}{dt} = \left\{ \begin{array}{l} 1.66\times 10^9 exp(-201.7/RT)\times \\ (1-x)[1-19.9ln(1-x)]^{1/2} \end{array} \right\} \quad (10)$$

where $x = \dfrac{W_0 - W}{W_0 - W_{ash}}$

with W_0, W are initial and present mass of char and W_{ash} is the mass of ash obtained from fuel analysis.

5. Gas phase reaction

The following five-step global gas phase reaction is considered [16].

$CH_4+H_2O \leftrightarrow CO+3H_2-206MJ/kmol$

$CH_4+1/2O_2 \leftrightarrow CO+2H_2+35.7MJ/kmol$

$H_2+1/2O_2 \leftrightarrow H_2O+242MJ/kmol$

$CO+1/2O_2 \leftrightarrow CO_2+283MJ/kmol$

$CO+H_2O \leftrightarrow CO_2+H_2+41.1MJ/kmol$

The reaction rates in the above are taken from the references [10] and [17]. The gas phase reaction is dominated either by chemical reaction or by turbulent mixing. The turbulent mixing rate is estimated in terms of integral time scale of turbulence. The problem domain is initialized with a relatively high temperature to ease the ignition process.

6. Prediction of NOx by CMC method

As already mentioned, fuel nitrogen evolves as HCN and NH_3. The split of this percentage of fuel nitrogen between HCN and NH_3 is a function of fuel type. Unless detailed information is available about the particular fuel it is recommended [9] to assume that all fuel nitrogen gets converted into HCN. Therefore in the present study it assumed that no NH_3 is formed from fuel nitrogen. With this only two more transport equations are to be solved, one for HCN and the other for NO.

$$\rho\frac{\partial Y_{HCN}}{\partial t} + \rho u_i \frac{\partial Y_{HCN}}{\partial x_i} = \frac{\partial}{\partial x_i}\left(\rho D \frac{\partial Y_{HCN}}{\partial x_i}\right) + \overline{W}_{HCN} \quad (11)$$

$$\rho\frac{\partial Y_{NO}}{\partial t} + \frac{\partial \rho u_i Y_{NO}}{\partial x_i} = \frac{\partial}{\partial x_i}\left(\rho D \frac{\partial Y_{NO}}{\partial x_i}\right) + \overline{W}_{NO} \quad (12)$$

The source terms for these transport equations are obtained as

$$\overline{W}_{NO} = (\overline{W}_1 - \overline{W}_2)M_{NO}$$
$$\overline{W}_{HCN} = (\overline{W}_0 - \overline{W}_1 - \overline{W}_2)M_{HCN} \quad (13)$$

where $\overline{W}_i$s are Favre mean formation or depletion rates calculated as follows.

$\overline{W}_0$ is the rate of formation of HCN from fuel nitrogen

$$\overline{W}_0 = \zeta \omega_N^{\nu} S_p^{\eta 1} / M_N \quad (14)$$

where ζ is the fraction of fuel nitrogen that goes to HCN, presently taken as unity. ω_N^{ν} is the mass fraction of nitrogen in the fuel. It is estimated as 0.0045 for this fuel. $S_p^{\eta 1}$ is the local source of particle mass given to the gas phase by devolatilization. $w_1(\eta)$ and $w_2(\eta)$ are calculated from formation and depletion of NO from HCN according to the following steps.

$$HCN + O_2 \rightarrow NO + \cdots\cdots \quad (15)$$

$$HCN + NO \rightarrow N_2 + \cdots\cdots \quad (16)$$

The conditional reaction rates of these reaction steps are calculated in mixture fraction space as

$$w_1(\eta) = A_1 X_{HCN} X_{O2}^b exp(-E_1/RT) \quad (17)$$

$$w_2(\eta) = A_2 X_{HCN} X_{NO} exp(-E_2/RT) \quad (18)$$

where X_i's represent the mole fractions of the corresponding species. The constants, A and E, are tabulated in [6, 9]. The reaction order, b, depends on oxygen concentration [6, 9].

To obtain the conditional reaction rates, information about the species concentrations in the mixture fraction space is needed. Here the mixture fraction is defined as the ratio of the amount of evaporated fuel to the total gas [15]. 40 mixture fraction grids are considered at each spatial grid point. Transport equations are solved for the mean and variance of mixture fraction to get local pdf's [12].

We estimate instantaneous mass fractions in the mixture fraction space from known Favre mean values as follows. It has been observed in many experimental works that a species reaction rate is only a function of local stoichiometry [2, 3]. The local instantaneous mass fractions Y_i are taken to be a linear function of its fully reacted mass fraction, Y_i^f.

$$Y_i = \pi_i Y_i^f \quad (19)$$

The value of π_i is the ratio of the Favre mean mass fraction at the flow grid to that of fully reacted equilibrium mass fraction. The Favre mean is obtained based on local beta pdf.

$$\pi_i = (\overline{Y}_i / \widetilde{Y_i^f}) \quad (20)$$

where

$$\widetilde{Y_i^f} = \int_0^1 Y_i^f(\eta) P(\eta) d\eta \quad (21)$$

With this information on instantaneous mass fractions we can calculate $w_1(\eta)$ and $w_2(\eta)$ in the mixture fraction space by Eqs. (17) and (18). Then the mean reaction rates are calculated as

$$\overline{W}_1 = \int_0^1 w_1(\eta) P(\eta) d\eta \quad (22)$$

and $$\overline{W}_2 = \int_0^1 w_2(\eta) P(\eta) d\eta \quad (23)$$

With these reaction rates proper source terms may be calculated and supplied to the equations (11) and (12).

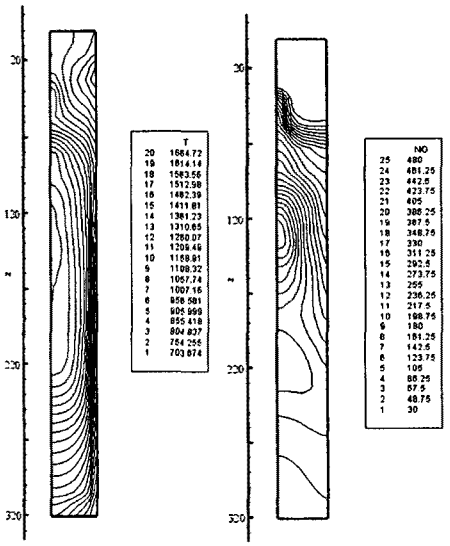

Fig 2. Steady state contour plots: Left: Temperature K, Right: NO mole fraction in PPM

7. Results and discussion

Numerical simulations are carried out for the different test cases in Table 1. Total heat loss along the wall is measured during experimental work at different axial locations. The measured heat flux values are implemented directly in numerical simulations.

Figure 2 shows the distributions of temperature and nitrogen oxide in the furnace in the steady state burning condition. Smooth contours of these parameters indicate sufficient grid resolution in these simulations.

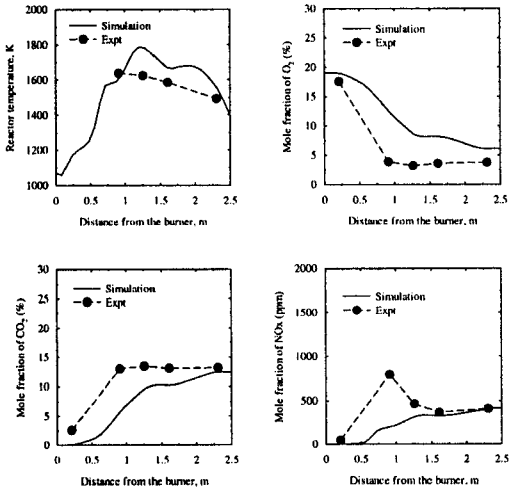

Fig 3. Variation along axial direction; data for the first graph are taken along the axis and data for the remaining graphs are extracted at r=80 mm (Test 1)

In experimental investigations gas samples are extracted in the axial direction along the axis and at r=80mm. The first graph in Fig 3. denotes distribution of temperature on the axis of the furnace along axial direction. Note that numerical predictions are in good agreement with those from experimental investigations. Mole fractions of O_2(in %), CO_2 (in %) and NO (in ppm) from numerical simulation are given in the last three graphs in Fig 3. These mole fractions are estimated after drying out of water vapor content. Mole fractions of O_2 and CO_2 reveal incomplete combustion in numerical simulation as compared with experimental observations. It may be noted that the NO level is around 400-500 ppm. Vacuum residue contains only a small percentage of nitrogen (0.45 %) and hence fuel NO percentage is much less than thermal NO. Even though the mean temperature is around 1800 K temperature fluctuations may go beyond 1800 K and hence support the production of significant thermal NO. These graphs show that the qualitative trend is captured, although there is some discrepancy in their absolute magnitudes. This discrepancy may be partly due to an improper SMD of injected droplets or an inaccurate model for devolatilization of vacuum residue.

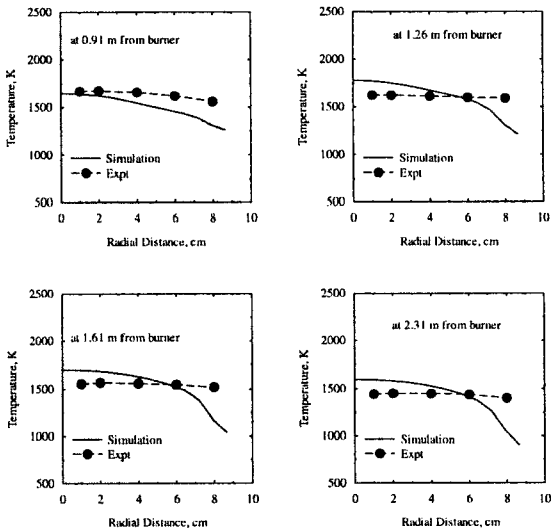

Fig 4. Variation of temperature along radial direction at four axial locations at axial distances of 0.91m, 1.26m, 1.61m and 2.31m from the burner (Test 1)

Radial profiles of temperature are extracted at four different axial locations 0.91m, 1.26 m, 1.61 m and 2.31 m from the tip of the burner. Simulation results are shown along with the experimental data in Fig 4. Note that these radial profiles are within an agreeable limit with experimental data at all locations.

Similar results were extracted for the test case 2 and are plotted in Figs. 5 and 6. Slightly higher temperatures are attained in this case compared to the previous test case with lower fuel flow rate. Better combustion

is achieved in test case 2 as compared with the test case 1. In test case 2 also a reasonable agreement is observed with experimental data.

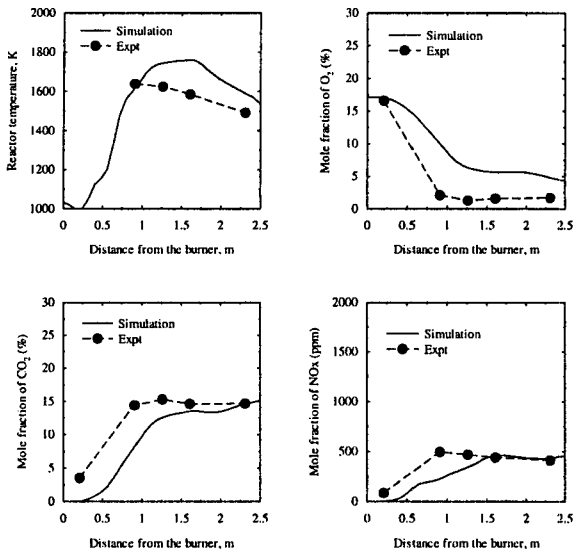

Fig 5. Variation along axial direction; data for the first graph are taken along the axis and data for the remaining graphs are extracted at r=80 mm (Test 2)

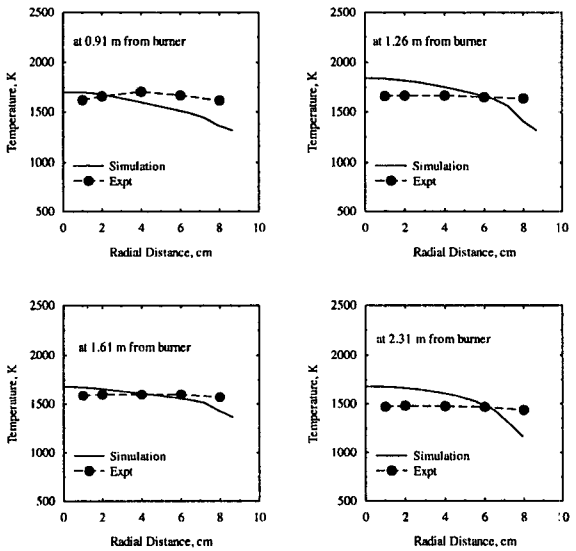

Fig 6. Variation of temperature along radial direction at four axial locations of axial distances of 0.91m, 1.26m, 1.61m, and 2.31m from the burner (Test 2)

8. Conclusion

Combustion of vacuum residue is investigated both experimentally and numerically in an experimental furnace. Combustion of vacuum residue is modeled in a similar way as that for pulverized coal particles. It goes through devolatilization, gas phase reaction and char oxidation. The CMC method is employed along with a decoupled flow solver to predict the NO levels. On the overall the numerical simulation results are in reasonable agreement with measured concentrations of major species, NO and temperature. It turns out that NO emission mainly comes from the thermal source for all operating conditions. Contribution of fuel NO contribution is much less because of a lower content of nitrogen in the fuel.

9. References

[1] Arthur J.A. (1951) Trans. Faraday Society, 47, 164

[2] Bilger R.W. (1979) Combustion Science and Technology, 19, 89

[3] Bilger R.W. (1980) Combustion Science and Technology, 22, 251

[4] Bowman C. T. (1975) Prog. Energy Combust. Sci. 1, 33

[5] Choi C.H. (2004) MS thesis, POSTECH, Korea

[6] Eaton A.M., Smoot L.D., Hill S.C. and Eatough C.N. (1999) Prog. Energy Combust. Sci. 25, 387

[7] Fujimura K, Mastumoto H, Arakawa Y, Fujii H and Mizoguchi T (1999) Development and operation results of VR firing boiler. Mitsubishi Juco Giho, Vol 36 No. 2 www.mhi.co.jp/tech/htm/9362/e936211a.htm

[8] Gray M.R. (1994) Upgrading petroleum residues and heavy oils, Marcel Dekker, Inc, New York

[9] Hill S.C. and Smoot L.D. (2000), Prog. Energy Combust. Sci. 26, 417

[10] Jones W. P. and Lindstedt R.P (1988) Combustion and Falme, 73, 233

[11] Klimenko A.Y. (1990), Fluid Dynamics (USSR) 25 327-334

[12] Libby P.A and Williams F.A (1994), in Turbulent reacting floes, Academic press,

London pp.2-61
[13] Malte P.C. and Pratt D.T. (1974) Combustion Science and Technology, 9, 221
[14] Minoru H. (1998) Demonstrative operation plan of asphalt burning power plant in oil refinery, 17th WEC congress, Huston, USA
[15] Smoot LD, editor. Fundamentals of coal combustion for clean and efficient use, Amsterdam: Elsevier (1993)
[16] Watanabe H., Otaka M., Hara S., Ashizawa M., Kidoguchi K., and Inumaru J., (2002) International Joint Power Generation Conference, Phoenix, AZ, USA.
[17] Westbrook C.K. and Dryer F.L (1981) Combustion Science and Technology, 27, 31
[18] Wolff J., Radtke K, Karg J and Gunster W. (2001) Refinery residue based on IGCC poerplants and market potential. Gasification technologies 2001 conference, San Francisco, CA